Supporting Information for "Past the precipice? Projected coral habitability under global heating"

P. Kalmus[1], A. Ekanayaka[2], E. Kang[2], M. Baird[3], and M. Gierach[1]

[1]Jet Propulsion Laboratory, California Institute of Technology, Pasadena, CA, USA

[2]University of Cincinnati, Cincinnati, OH, USA

[3]CSIRO, Oceans and Atmosphere, Hobart, Australia

Contents of this file

Introduction

This Supporting Information contains additional supporting text, additional supporting figures, and additional supporting tables for our paper.

Text S1.

Here we describe the empirical determination of the sensitivity of departure year to the DHW threshold and to the climatological baseline on which it is referenced for SSP245, SSP370, and SSP585, from which we can derive the direct equivalence relationship between DHW threshold and climatological baseline. To do this, we began by defining five climatological reference periods, 15 year contiguous period centered around 1970, 1980, 1990, 2000, and 2010. Since we required more than two decades of time span in which to perform this experiment, and the MUR SST dataset only goes back to 2002, we used the HadISST observational dataset, which has a horizontal resolution of 1 degree, and the global model ensemble of SST projections at the same spatial resolution. We calculated HadISST climatologies at each reef-containing coarse grid point. We did this for SSP245, SSP370, and SSP585. We did not include SSP126 due to the many reef locations which depart only after 2100.

For these three climate scenarios, and for each of the five climatological baselines, we find the year of projected departure beyond a threshold of 8 DHW at an annual return frequency at each 1-degree reef-containing grid cell. We then find the mean value over all the grid cells for each scenario and climatological baseline, and determine the least squares linear fit for each scenario (Figure S1, first column). We next perform a similar experiment, except instead of varying the climatological baseline, we choose one baseline (2010, i.e. 2003-2017) and vary the DHW threshold (Figure S1, second column). This determines an empirical relationship between the climatological baseline and the DHW threshold.

While the mean departure years from each of the three SSPs have different linear relationships to climatological baseline and DHW threshold, we find that the climatologically adjusted DHW threshold is 4.8 for each climate scenario. The largest difference between the three pairs of numbers (0.05 DHW) corresponds to mean departure year errors of 0.11 years, 0.14 years, and 0.20 years for SSP585, SSP370, and SSP245 respectively. These errors are negligible compared to other uncertainties in the analysis. We can use these relationships to determine equivalent DHW thresholds for any climatological baseline.

Text S2.

The following model groups and model members were used to produce Tables S1 and S2 below, using the methods described in the paper:

ACCESS-CM2 r1i1p1f1, ACCESS-CM2 r2i1p1f1, ACCESS-CM2 r3i1p1f1, ACCESS-ESM1-5 r1i1p1f1, ACCESS-ESM1-5 r2i1p1f1, ACCESS-ESM1-5 r3i1p1f1, BCC-CSM2-MR r1i1p1f1, CAMS-CSM1-0 r1i1p1f1, CAMS-CSM1-0 r2i1p1f1, CESM2 r10i1p1f1, CESM2 r11i1p1f1, CESM2 r4i1p1f1, CESM2-WACCM r1i1p1f1, CMCC-CM2-SR5 r1i1p1f1, CNRM-CM6-1 r1i1p1f2, CNRM-CM6-1 r2i1p1f2, CNRM-CM6-1 r3i1p1f2, CNRM-CM6-1 r4i1p1f2, CNRM-CM6-1 r5i1p1f2, CNRM-CM6-1 r6i1p1f2, CNRM-CM6-1-HR r1i1p1f2, CNRM-ESM2-1 r1i1p1f2, CNRM-ESM2-1 r2i1p1f2, CNRM-ESM2-1 r3i1p1f2, CNRM-ESM2-1 r5i1p1f2, CanESM5 r10i1p1f1, CanESM5 r10i1p2f1, CanESM5 r11i1p1f1, CanESM5 r11i1p2f1, CanESM5 r12i1p1f1, CanESM5 r12i1p2f1, CanESM5 r13i1p1f1, CanESM5 r13i1p2f1, CanESM5 r14i1p1f1, CanESM5 r14i1p2f1, CanESM5 r15i1p1f1, CanESM5 r15i1p2f1, CanESM5 r16i1p1f1, CanESM5 r16i1p2f1, CanESM5 r17i1p1f1, CanESM5 r17i1p2f1, CanESM5 r18i1p1f1, CanESM5 r18i1p2f1, CanESM5 r19i1p1f1, CanESM5 r19i1p2f1, CanESM5 r1i1p1f1, CanESM5 r1i1p2f1, CanESM5 r20i1p1f1, CanESM5 r20i1p2f1, CanESM5 r21i1p1f1, CanESM5 r21i1p2f1, CanESM5 r22i1p1f1, CanESM5 r22i1p2f1, CanESM5 r23i1p1f1, CanESM5 r23i1p2f1, CanESM5 r24i1p1f1, CanESM5 r24i1p2f1, CanESM5 r25i1p1f1, CanESM5 r25i1p2f1, CanESM5 r2i1p1f1, CanESM5 r2i1p2f1, CanESM5 r3i1p1f1, CanESM5 r3i1p2f1, CanESM5 r4i1p1f1, CanESM5 r4i1p2f1, CanESM5 r5i1p1f1, CanESM5 r5i1p2f1, CanESM5 r6i1p1f1, CanESM5 r6i1p2f1, CanESM5 r7i1p1f1, CanESM5 r7i1p2f1, CanESM5 r8i1p1f1, CanESM5 r8i1p2f1, CanESM5 r9i1p1f1, CanESM5 r9i1p2f1, CanESM5-

CanOE r1i1p2f1, CanESM5-CanOE r2i1p2f1, CanESM5-CanOE r3i1p2f1, EC-Earth3 r11i1p1f1, EC-Earth3 r15i1p1f1, EC-Earth3 r1i1p1f1, EC-Earth3 r4i1p1f1, EC-Earth3-Veg r1i1p1f1, EC-Earth3-Veg r2i1p1f1, EC-Earth3-Veg r3i1p1f1, EC-Earth3-Veg r4i1p1f1, FGOALS-f3-L r1i1p1f1, FGOALS-f3-L r2i1p1f1, FGOALS-f3-L r3i1p1f1, FGOALS-g3 r1i1p1f1, FGOALS-g3 r2i1p1f1, FGOALS-g3 r3i1p1f1, FGOALS-g3 r4i1p1f1, GFDL-ESM4 r1i1p1f1, GISS-E2-1-G r1i1p3f1, IPSL-CM6A-LR r14i1p1f1, IPSL-CM6A-LR r1i1p1f1, IPSL-CM6A-LR r2i1p1f1, IPSL-CM6A-LR r3i1p1f1, IPSL-CM6A-LR r4i1p1f1, IPSL-CM6A-LR r6i1p1f1, MCM-UA-1-0 r1i1p1f2, MIROC-ES2L r1i1p1f2, MIROC6 r1i1p1f1, MIROC6 r2i1p1f1, MIROC6 r3i1p1f1, MPI-ESM1-2-HR r1i1p1f1, MPI-ESM1-2-HR r2i1p1f1, MPI-ESM1-2-LR r10i1p1f1, MPI-ESM1-2-LR r1i1p1f1, MPI-ESM1-2-LR r2i1p1f1, MPI-ESM1-2-LR r3i1p1f1, MPI-ESM1-2-LR r4i1p1f1, MPI-ESM1-2-LR r5i1p1f1, MPI-ESM1-2-LR r6i1p1f1, MPI-ESM1-2-LR r7i1p1f1, MPI-ESM1-2-LR r8i1p1f1, MPI-ESM1-2-LR r9i1p1f1, NorESM2-LM r1i1p1f1, NorESM2-MM r1i1p1f1, UKESM1-0-LL r1i1p1f2, UKESM1-0-LL r2i1p1f2, UKESM1-0-LL r3i1p1f2, UKESM1-0-LL r4i1p1f2, UKESM1-0-LL r8i1p1f2, INM-CM4-8 r1i1p1f1, INM-CM5-0 r1i1p1f1.

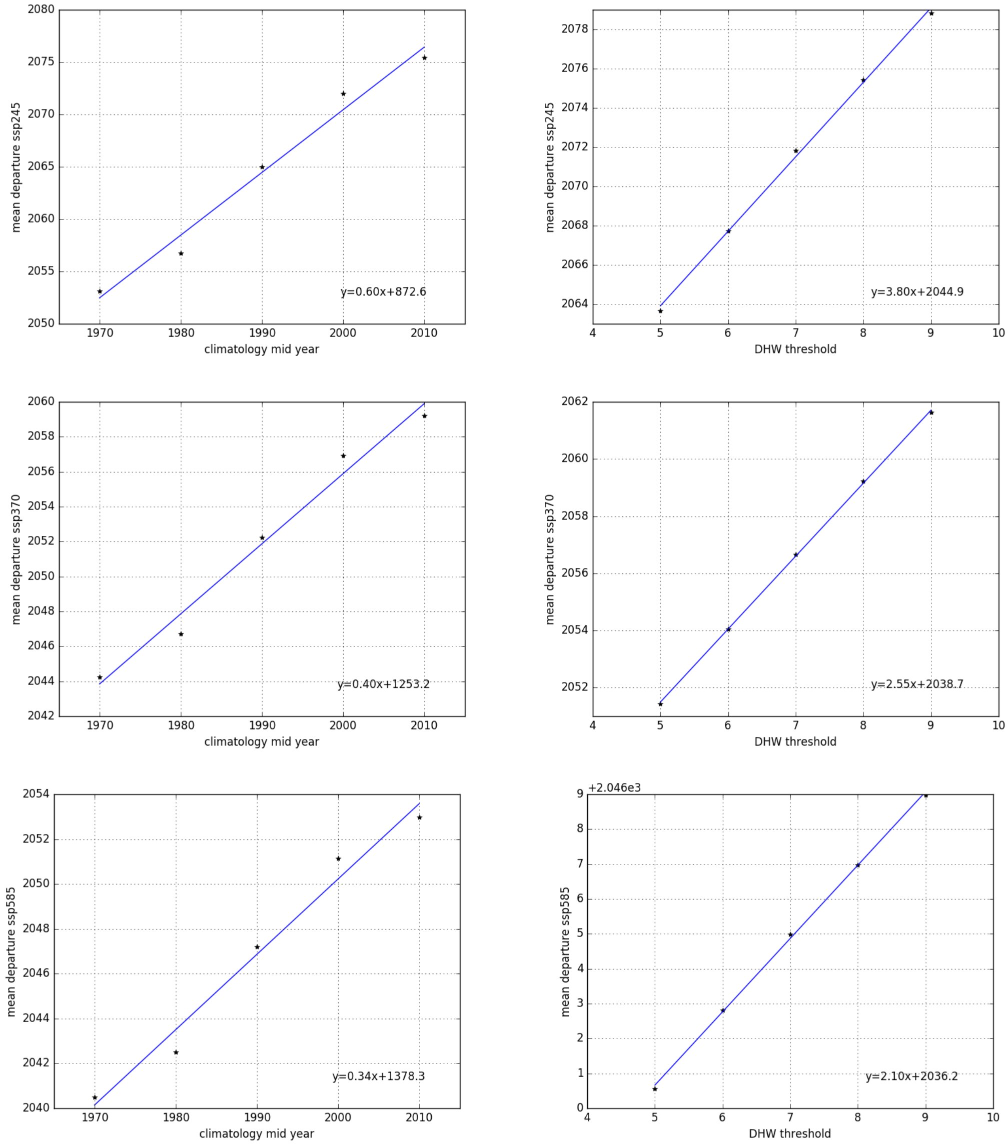

Figure S1. Departure year sensitivity to climatology center year (left) and degree heating weeks (right) for SSP245 (top row), SSP370 (middle row) and SSP585 (bottom row).

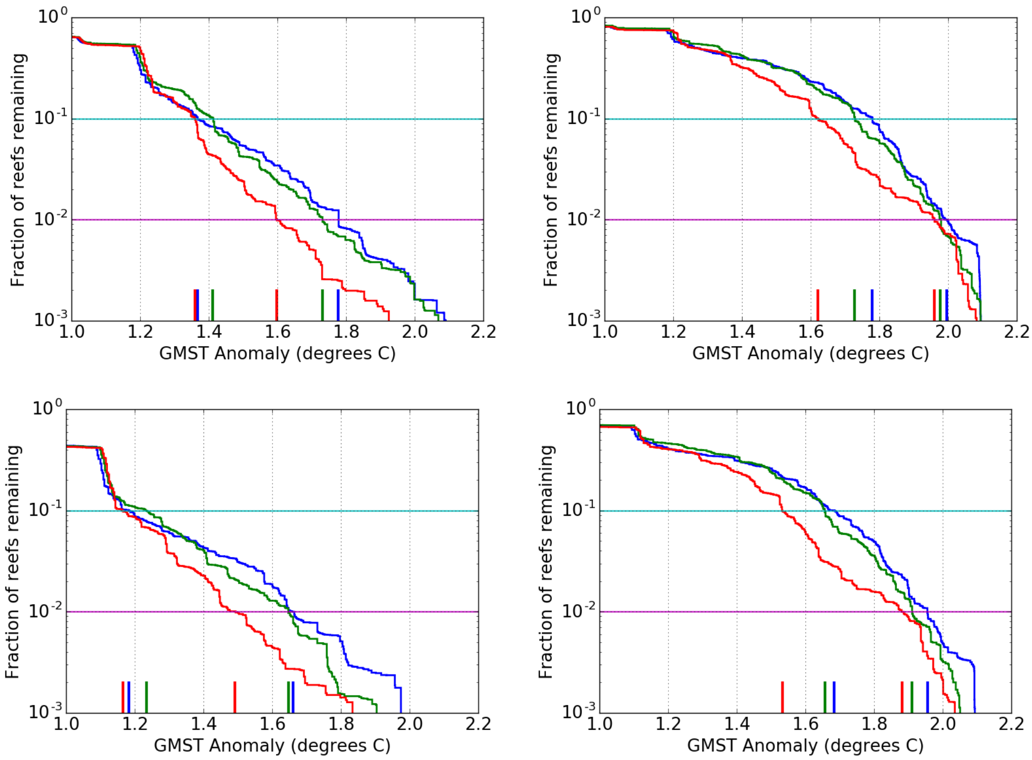

Figure S2. Cumulative histograms of thermal departure as a function of GMSTA, for SSP126 (black), SSP245 (blue), SSP370 (green), SSP585 (red), for a five year heat event return timescale (TD5Y, top row) and a ten year heat event return timescale (TD10Y, bottom row). Both DHW thresholds are shown. Cyan and magenta horizontal lines show the 10% and 1% fractional levels respectively; colored vertical ticks on the y-axis indicate crossings of these levels. Shading indicates the propagated MUR SST uncertainty.

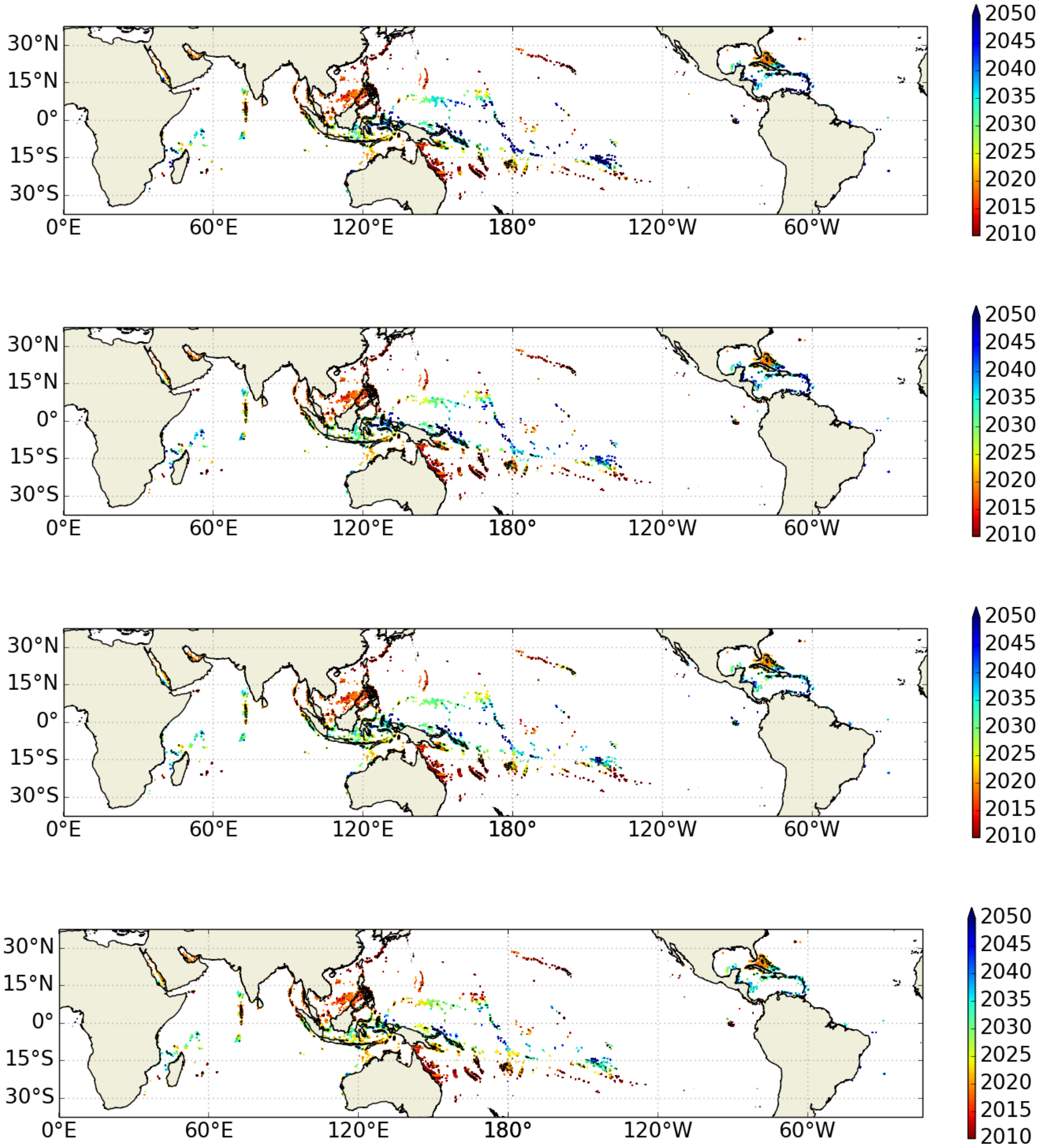

Figure S3. Global maps of thermal departure under the four emissions scenarios (from top: SSP126, SSP245, SSP370, SSP585) for TD5Y and the 8 DHW_{2008} threshold.

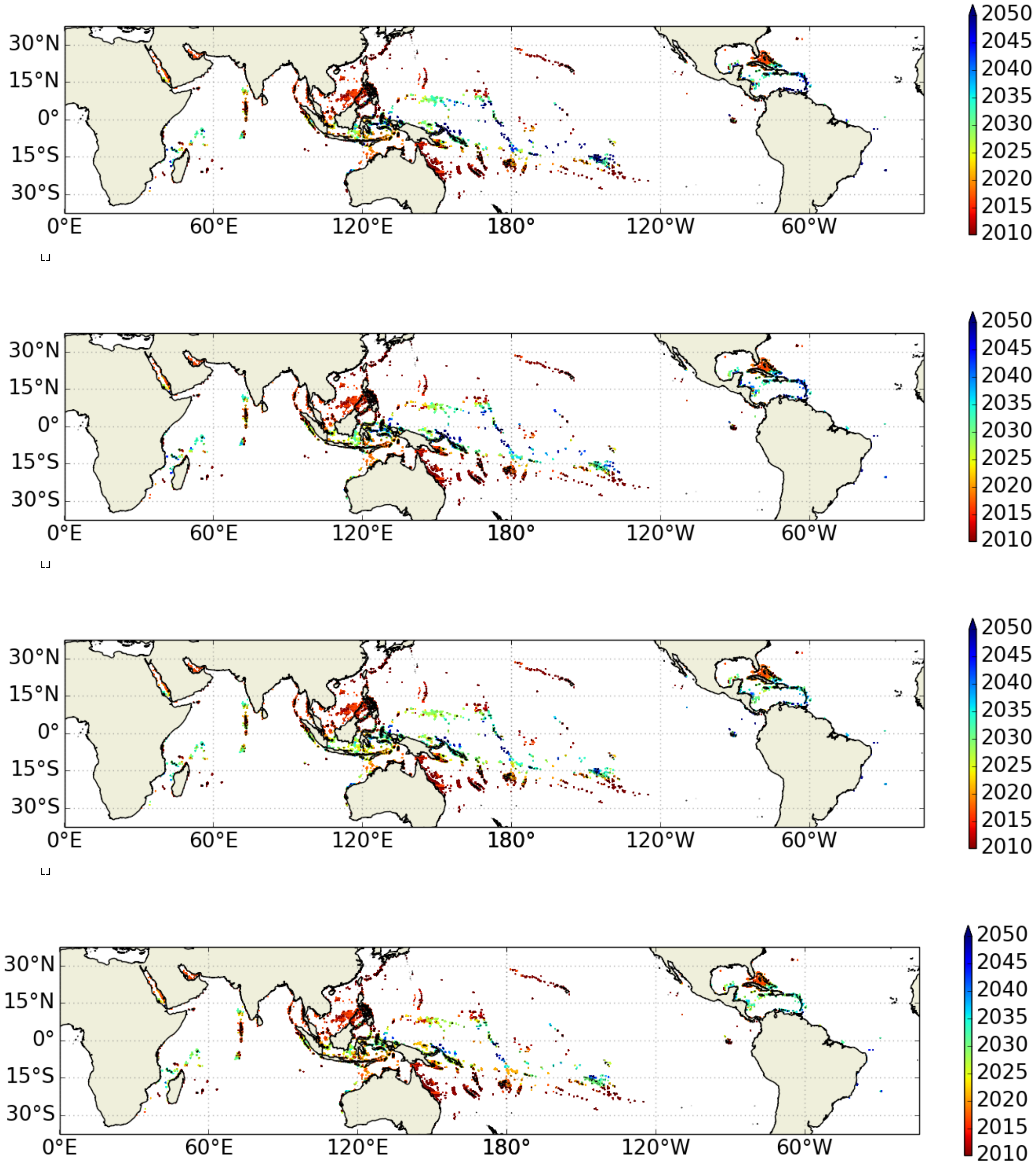

Figure S4. Global maps of thermal departure under the four emissions scenarios (from top: SSP126, SSP245, SSP370, SSP585) for TD10Y and the 8 DHW_{2008} threshold.

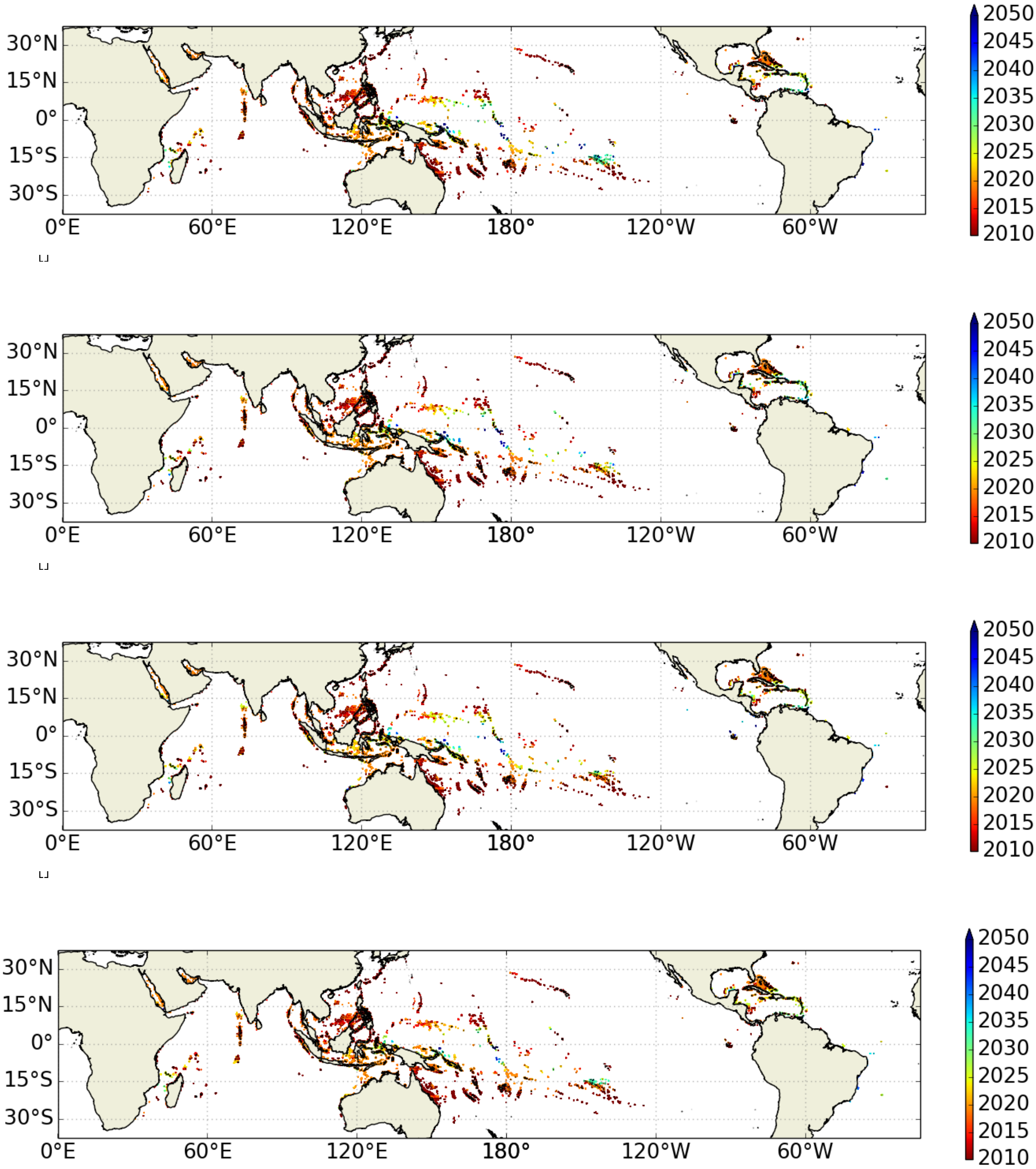

Figure S5. Global maps of thermal departure under the four emissions scenarios (from top: SSP126, SSP245, SSP370, SSP585) for TD5Y and the 8 DHW_{1988} threshold.

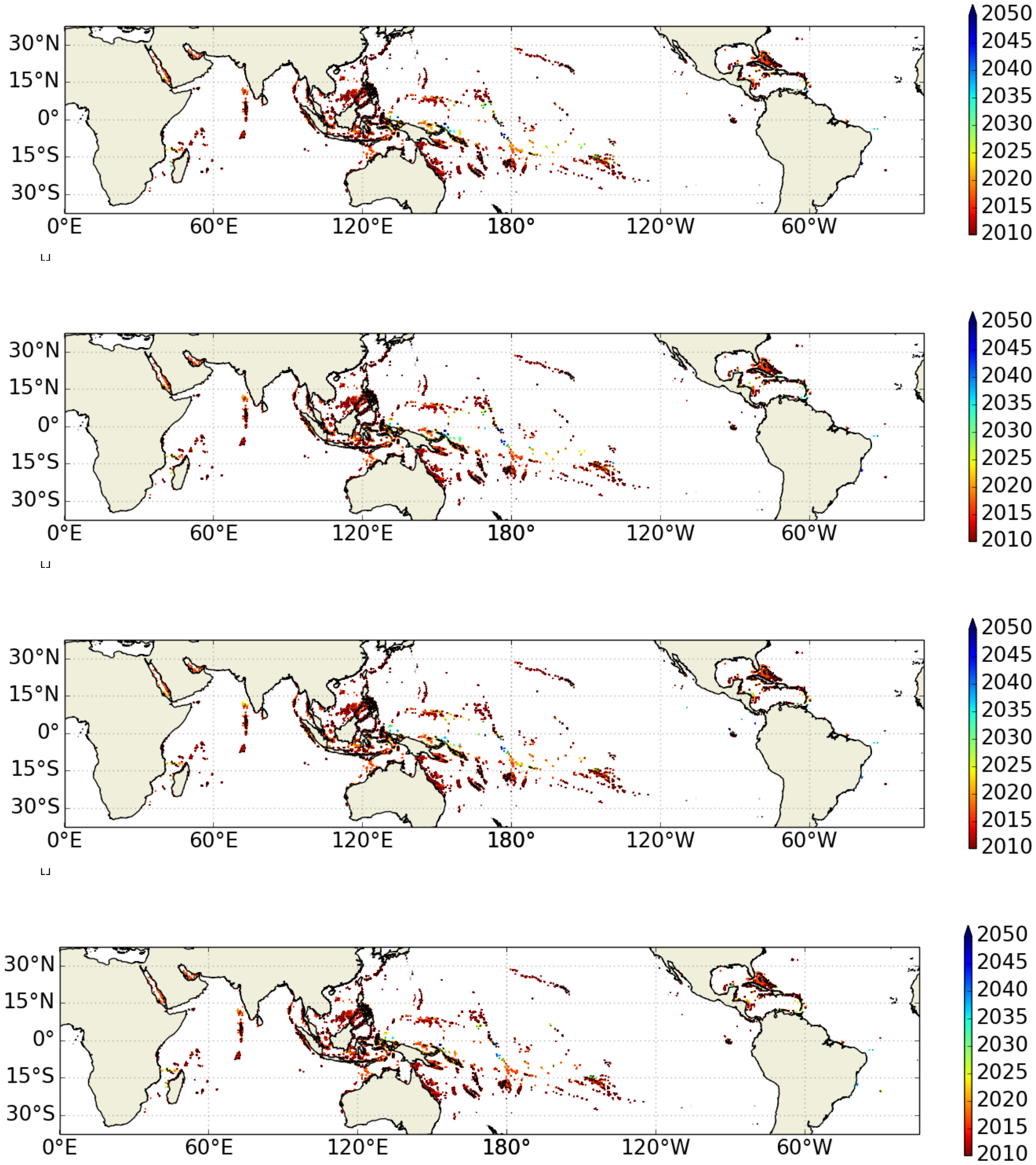

Figure S6. Global maps of thermal departure under the four emissions scenarios (from top: SSP126, SSP245, SSP370, SSP585) for TD10Y and the 8 DHW_{1988} threshold.

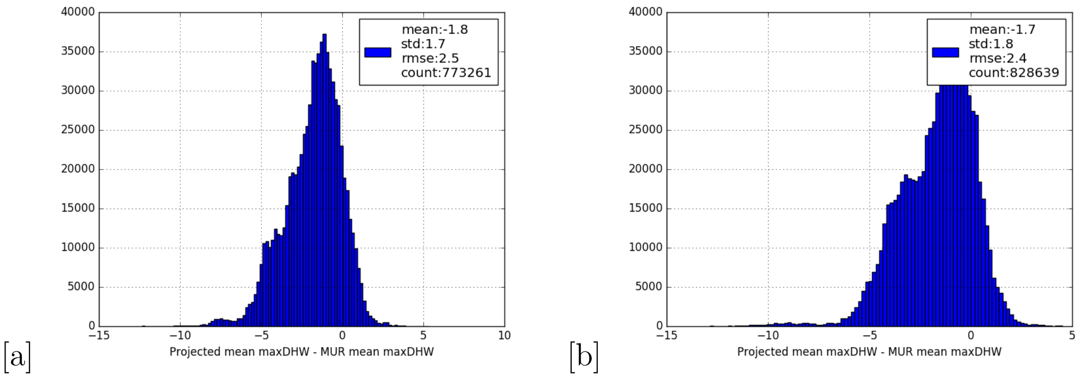

Figure S7. Error distributions of the mean of the three annual maximum DHW values calculated between 2018 and 2020 from MUR subtracted from the corresponded value from the downscaled model ensemble, for SSP126 and using (a) the CMIP6 model ensemble used in the paper with 35 model members; (b) The CMIP6 model ensemble listed in Supplemental Information T2 with 127 model members.

Table S1. Projected years and GMSTAs after which fewer than the stated percentage of 1 km^2 reef locations remain below the thermal thresholds, using the models and model members listed in Text S2 and methods described in the paper

	5Y 8 DHW_{2008}			10Y 8 DHW_{2008}			5Y 8 DHW_{1988}			10Y 8 DHW_{1988}		
SSP	30%	10%	1%	30%	10%	1%	30%	10%	1%	30%	10%	1%
Year in twenty-first century												
126	26	90	-	23	37	-	19	23	-	16	18	86
245	26	36	69	22	33	58	19	21	41	16	17	34
370	26	34	50	22	31	44	19	22	35	16	17	32
585	24	33	47	20	30	43	19	21	33	16	17	30
Global mean surface temperature anomalies (degrees C)												
245	1.4	1.7	2.0	1.3	1.6	2.0	1.2	1.3	1.8	1.1	1.1	1.6
370	1.4	1.7	2.0	1.3	1.6	1.9	1.2	1.3	1.7	1.1	1.2	1.6
585	1.4	1.6	2.0	1.3	1.5	2.0	1.2	1.3	1.6	1.1	1.1	1.5

Table S2. Percentages and numbers of reef locations remaining below the stated GMSTA value (in degrees C) for a given bleaching metric, using the models and model members listed in Text S2 and methods described in the paper

	5Y 8 DHW_{2008}			10Y 8 DHW_{2008}			5Y 8 DHW_{1988}			10Y 8 DHW_{1988}		
SSP	1.5	1.7	2.0	1.5	1.7	2.0	1.5	1.7	2.0	1.5	1.7	2.0
Percent 1 km^2 reef locations remaining below GMSTA value												
245	26%	10%	1%	19%	7%	1%	4%	1%	0%	2%	1%	0%
370	24%	8%	1%	16%	6%	0%	3%	1%	0%	2%	1%	0%
585	15%	5%	1%	11%	3%	1%	2%	1%	0%	1%	0%	0%
Number of 1 km^2 reef locations remaining below GMSTA value, out of 829K												
245	213K	79K	10K	161K	59K	5350	30K	11K	1796	18K	5615	384
370	205K	74K	14K	139K	51K	6248	30K	10K	1983	19K	5090	717
585	136K	51K	16K	98K	29K	8005	16K	5117	1365	10K	3102	946